Coherent transport and symmetry breaking—laser dynamics of constrained granular matter

Coherent transport and symmetry breaking—laser dynamics of constrained granular matter

Andreas Lubatsch[1] **and Regine Frank**[2,3,4]

[1] Electrical Engineering, Precision Engineering, Information Technology, Georg-Simon-Ohm University of Applied Sciences, Kesslerplatz 12, 90489 Nürnberg, Germany
[2] Institute of Theoretical Physics, Optics and Photonics, Auf der Morgenstelle 14, Eberhard-Karls-Universität, 72076 Tübingen, Germany
[3] National Center of Theoretical Physics (NIThep), Stellenbosch University, Matieland 7602, South Africa
[4] Institute of Solid State Physics, Wolfgang-Gaede Strasse 1, Karlsruhe Institute of Technology (KIT), 76131 Karlsruhe, Germany
E-mail: r.frank@uni-tuebingen.de

Abstract

We present diagrammatic transport theory including self-consistent nonlinear enhancement and dissipation in the multiple scattering regime. Our model of Vollhardt–Wölfle transport of photons is fit-parameter-free and raises the claim that the results hold up to the closest packed volume of randomly arranged ZnO Mie scatterers. We find that a symmetry breaking caused by dissipative effects through the lossy underlying silicon (SI) substrate leads to qualitatively different physics of coherence and lasing in granular amplifying media. According to our results, confined and extended random laser modes and their laser thresholds can be clearly attributed to unbroken and broken spatial symmetry. The diameters and emission profiles of the modes, as well as their thresholds and the positional-dependent degree of coherence, can be checked experimentally.

Keywords: random lasers, transport of light, theory, nonlinearity, symmetry breaking, complex systems, multiple scattering, Bethe–Salpeter equation

1. Introduction

After two decades of random laser research [1–6] these systems are still highly fascinating. The involved rich physics and also possible applications [7, 8] in systems that, at first glance, appear to be just 'dust powder' have started to reveal more and more fascinating details. Absolutely essential for the fundamental behavior of a random laser is the spatial extension of random lasing modes. If the lasing spots are strongly confined, the random laser is actually operated as a collection of single-mode lasers where the modes do not overlap in space [9, 10]. On the other hand, the random laser can exhibit another type of mode which covers the whole ensemble showing significantly different emission characteristics and a higher laser threshold. Additionally all these properties are derived without a confining external resonator and the modes seem to be due only to transport through disordered granular media and amplification. The experimental finding that spatially confined and extended laser modes can actually co-exist in the same region of strongly scattering nano-crystalline powders [11, 12] has been completely counterintuitive. Nevertheless an *ab initio* description for coherent emitting modes in diffusive, weakly or strongly localizing systems could not yet be given for this phenomenon. In this paper we derive, by means of quantum field diagrammatical photon transport incorporating several loss channels, spatially confined and extended random laser modes which may co-exist. It is proven that the experimentally observed mode types in different gain regimes can be explained in a single framework of transport renormalized by dissipation. Dissipation processes are not only frequency selective with respect to the absorption and transmission properties of the substrate, they can be further influenced by the dispersity of the powder, and they are coupled to the nonlinear enhancement. We show that the emission statistics, the coherence and the threshold of random laser modes are severely changing due to symmetry breaking of photonic transport by dissipation. However we find that modes with strong losses also arrive at a laser threshold. This result can be checked by measuring the extent and the degree of coherence of random laser modes relying on non-symmetric boundaries.

2. Light in granular matter

In non-linear granular systems of low filling fraction, photonic transport obeys the well known diffusion equation, whereas in densely packed random media coherent transport sets in which is foremost seen in a deviation from the exponential decay of diffusive light intensity, or the long-time tail. Fancy effects such as coherent backscattering (CBS), a factor of two of light intensity in the exact backscattering direction, can be observed. Diagrammatic transport of light intensity, which treats light propagation as well defined paths of photons (see figure 1), can describe these observations. A photon (green line) is scattered by active particles, or possible spheres. This means that it is absorbed by a particle and excites the electronic structure of the material as well as the internal geometrical resonance, Rayleigh-scattering or Mie-scattering. During the (re-) emission process, the frequency conversion and decoherence processes of the electronic sub-structure can lead to frequency changes. The exact time reversal procedure is denoted in red. Both photons, the forward propagator and the time reversal procedure can interfere. A perfect interference or correlation of the propagator and time-reversal procedure is represented in diagrammatics by the most crossed diagram, the Cooperon [13, 14]. Cooperons again may suffer destructive influences at the sample boundaries. If photons leak out or if their frequency
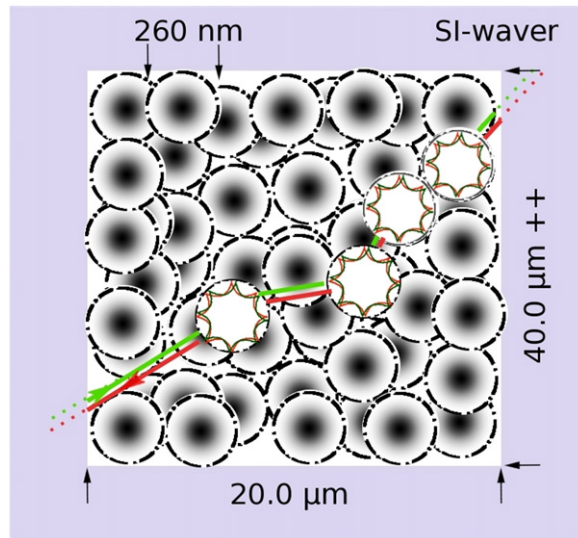
Figure 1. Schematic setup of ZnO nano grains embedded in a SI-waver. The spheres' diameter is $d = 260\,nm$. The samples' size is assumed to be $20.0\,\mu m \times 40.0\,\mu m++$. The non-quadratic size is assumed to show the symmetry breaking due to a high aspect ratio and lossy SI boundary. The sample extent is $4.0\,\mu m$ in the third dimension. The volume filling is 50%. Far below the laser threshold the permittivity of ZnO is given by $Re\,\epsilon_s = 4.0164$. Red and green paths represent counter-propagating, time reversal, photons coupled in non-linear response of ZnO and the complex Mie resonance of the wave.

is absorbed, the symmetry is broken. Absorption processes anywhere in the setup can be efficiently used to tune light transport in random systems as well as in waveguides [15].

Lasing in granular media is often described in terms of random cavities [16] modes or quasi-(leaky) modes [17]. These modes are by definition coherent and therefore obey Poissonian statistics. They have been estimated to form artificial but random cavities which are determined by the local scatterer arrangement. This scenario is of course possible, but fundamentally different from what we describe in this letter.

We investigate with the diagrammatic ansatz random lasing in nanocrystalline ZnO samples embedded in small depressions etched in a Si waver. A similar experimental setup can be found in [11]. It has been found that at the first laser threshold a spatially confined mode starts to lase symmetrically in space. With increasing pump strength, a rising number of modes of this type may be found strongly localized at several spatial positions. Increasing the excitation power further, a second laser threshold for a different lasing frequency of another type of mode is found. The diameter of this mode is large compared to the others; it may even cover the whole sample. The physics of both modes is fundamentally different and we will see that the extended mode arises in principle only in response to a symmetry breaking caused by locally occurring dissipation at the boundaries (see figure 1).

3. Coherent photon transport

We use a diagrammatic field theory ansatz for light in a diffusive system including interferences, the Vollhardt–Wölfle theory of photons [18, 19], which has proven to be rigorous for signatures of Anderson localization in non-linear random media [20]. *Vollhardt–Wölfle*

ansatz precisely means that the modes we derive here are in their information value not restricted to the coherence of the wave, but that they additionally describe the coherence of transported light intensity and it's decay. As already outlined the difference in the diameters cannot be explained solely by the increase of the pump power or the dispersity of the powder alone. Only when investigating frequency dependent dissipation varying in space, the absorption of photons by the crystal substrate at the boundaries does in fact yield the difference of the diameters. Loss initially suppresses a large number of modes which only eventually arrive at their lasing threshold for significantly higher pump strengths when the intrinsic nonlinear gain yields a balanced process. Strictly speaking, several spatially and spectrally distinctive loss channels within the ZnO sample and the Si crystal substrate [21] lead to the coexistence of both types of modes; the extended mode overall loses more intensity. It seems at first sight that the principle itself is reprising at another intensity scale which is induced by further degrees of freedom, but the study of the correlation length with respect to the position in the granular matter will clearly bring forward that symmetry breaking due to loss causes fundamental differences. One could even imagine tuning the powder's parameters in such a way that a stepwise access to different loss mechanisms could be possible and the random laser therefore could be controlled by the ensemble size, the surface, the type of substrate etc.

Theoretically the non-linearity is actually being established by doubly nested self-consistent computing. In the following a description for correlation and coherence of light in terms of wave and particle is explained. The photon density response, the four-point correlator, is derived from Bethe–Salpeter equation (BS) for photons,

$$\Phi = G^R G^A \left[1 + \int \frac{d^3q}{(2\pi)^3} \gamma \Phi \right] \tag{1}$$

which reads in position space

$$\Phi\left(r_1, r_1'; r_2, r_2'\right) = \; G^R\left(r_1, r_1'\right) G^A\left(r_2, r_2'\right)$$
$$+ \sum_{r_3, r_4, r_5, r_6} G^R(r_1, r_5) G^A(r_2, r_6) \gamma(r_5, r_3; r_6, r_4) \Phi\left(r_3, r_1'; r_4, r_2'\right). \tag{2}$$

The numbering marks independent positions within space, while the dashes denote the self-consistency of the diagram. All interference effects are considered by means of the irreducible vertex γ which includes most crossed diagrams (Cooperons) yielding memory effects as well as retardation, and it finally causes second order coherent emission of random lasers. From BS a Boltzmann equation is derived which yields two independent equations, namely the continuity and the current density relation. Local energy conservation is guaranteed by means of a Ward identity (WI). The sample is modeled by a system which is large (infinitely) sized in one direction but finite otherwise. The Fourier transform in the infinite direction x of equation (2), and use of the expression for the single particle Green's function $G = [\epsilon_b(\omega/c)^2 - |\mathbf{q}|^2 - \Sigma_{\mathbf{q}}^\omega]^{-1}$, leads to the kinetic equation for the correlator Φ with spatial dependencies due to the additional loss channels at the boundaries of the finite y-direction,

$$\left[\Delta\Sigma + 2\text{Re}\,\epsilon_b\omega\Omega - 2\text{Im}\,\epsilon_b\omega^2 - 2\overrightarrow{P_x}\cdot\overrightarrow{Q_X} + 2ip_y\partial_Y\right]\Phi_{pp'}^{Q_X}(Y, Y')$$

$$= \Delta G_p(Q_X; Y, Y')\delta(p - p')$$

$$+ \sum_{Y_{3,4}}\Delta G_p(Q_X)\int\frac{\mathrm{d}p''}{(2\pi)^2}\gamma_{pp''}^{Q_X}\left(Y, Y_{3,4}\right)\Phi_{p''p'}^{Q_X}\left(Y_{3,4}, Y'\right). \qquad (3)$$

$\Delta G = G^R - G^A$, p, p' and p'' are momenta. The scatterer's geometric properties are represented within the Schwinger–Dyson (SD) equation $G = G_0 + G_0 TG$ which leads to the solution for the Green's function G^R and G^A of the electromagnetic field, i.e. the light wave. Extended amplifying Mie spheres [22] as scattering centers [23] are represented by the self-consistent complex valued scattering matrices T leading to the self-energy Σ, which is derived in the independent scatterer approximation here. The ZnO scatterer's initial permittivity is given by $Re\,\epsilon_s = 4.0164$, while the imaginary part $Im\,\epsilon_s$, the microscopic gain, is derived self-consistently in what follows, yielding saturation effects. The background medium is air $\epsilon_b = 1$. The photon density emitted from the amplifying Mie particles is derived by means of coupling to a rate equation system. It is therefore self-consistently connected to nonlinear gain and the dielectric function $\epsilon = \epsilon_L + \epsilon_{NL}$. The latter finally yields nonlinear feedback in both electromagnetic wave transport (SD frame) and intensity transport (BS frame).

Dissipation processes at the boundaries severely influence the Green's functions, formalism. It is well known that Green's functions, intended to describe the transport of photons in the random laser on the one hand but being a description of microcanonical ensembles on the other hand, have to obey time reversal invariance. However within grand canonical (open) ensembles of random lasers the entropy is increased by photonic intensity transport processes which nevertheless obey time reversal symmetry for the propagation of the electromagnetic wave in between the active scatterers. This aspect of dissipation and disorder guarantees the completeness of the *ab initio* description of the propagating light intensity by the four-point correlator $\Phi = A\,\Phi_{\epsilon\epsilon} + B\,\Phi_{J\epsilon}$ here given in terms of the momenta: $\Phi_{\epsilon\epsilon}$ equals the energy density and $\Phi_{J\epsilon}$ equals the energy current, while A and B are pre-factor terms derived in [18]. Starting with the renormalized scattering mean free path l_s, the framework yields all relevant transport lengths and includes all interference effects. The modal behavior, the core of the random laser, is described efficiently by the determination of the correlation length ξ with respect to various spatially dependent loss channels. The coexistence of strongly confined and extended modes can be consistently explained. BS is solved in a sophisticated regime of real space and momentum with respect to the high aspect ratio of the random laser sample, and the description for the energy density $\Phi_{\epsilon\epsilon}(Q, \Omega)$ is derived, with regard to energy conservation, as follows:

$$\Phi_{\epsilon\epsilon}(Q, \Omega) = \frac{N_\omega(Y)}{\Omega + iDQ_X^2 \underbrace{-iD\chi_d^{-2} - c_1\left(\partial_Y^2\Phi_{\epsilon\epsilon}(Q, \Omega)\right) + c_2 + iD\zeta^{-2}}_{iD\xi^{-2}}}. \qquad (4)$$

Here the numerator N_ω basically represents the local density of photonic modes LDOS which is sensitive to amplification and absorption of the electromagnetic wave. Q is the center of mass momentum of the propagator denoted in Wigner coordinates, the index denotes the Fourier partner. Ω is the center of mass frequency and D is the self-consistently derived diffusion constant. c_1, c_2 are coefficients explained in [18].
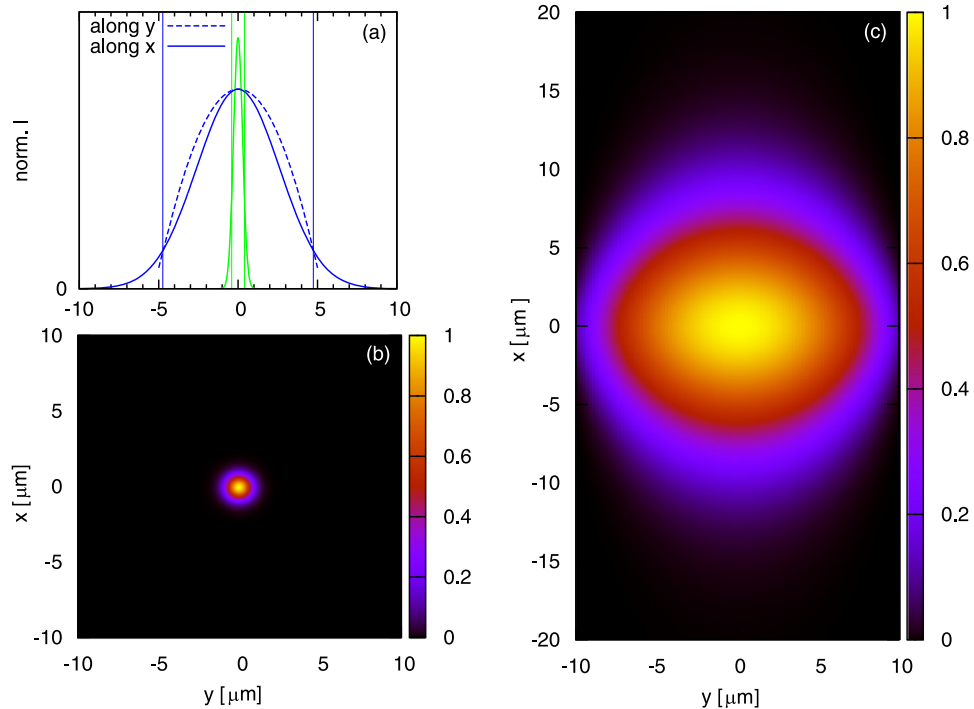
Figure 2. Computed lasing mode diameters and intensity distribution (color bar). Samples parameters can be found in figure 1. Results are shown for homogeneous 2 photon pumping $\lambda = 355$ nm (bulk ZnO bandedge). (a) Comparison of the intensity profile through the mode center for the symmetric confined mode (green) and the extended mode (blue lines, taken along x- and y-direction) at threshold. Vertical lines represent the decay to $1/e$ compared to the modes maximum intensity. Both modes are spectrally separated as explained in the text. Corresponding laser dynamics are shown in figure 4. (b) Confined mode, unbroken symmetry. Emission energy is 3.23 eV, the transport mean free path $l_s = 499.2$ nm. (c) Extended mode, broken symmetry. Emission energy 3.21 eV, $l_s = 501.57$ nm. The color gradient denotes the absolute amount of coherently emitted lasing intensity with its spatial dependency.

The equation for the energy density Φ, equation (4), represents a new result describing the propagation of photons within a finite sample. This is in contrast to previous work where the results were derived solely in momentum space for infinite sized systems. Here we follow methodologically the systematically outlined transport scheme in [18] but we additionally take into account the spatial dependence as denoted in equation (3) and displayed in figure 1: the sample shall be homogeneously pumped from above. Diffusive transport, especially interferences, occur preferentially on long paths in-plane of the large scaled random laser sample. The physics of most crossed diagrams therefore significantly dominates the coherence properties: dissipation and losses due to spontaneous emission and non-radiative decay are basically homogeneous, however at the sample's edges the situation changes qualitatively. Here transport is inhibited and photons are absorbed within the SI substrate. This frequency selective dissipation severely affects the spectrum of lasing modes and their diameters. All these channels are represented within the pole of equation (4) resulting in separate dissipative length scales ζ due to homogeneous losses (figure 2(b)), and χ_d due to gain and absorption that go along with photonic transport and the open or strongly absorbing SI
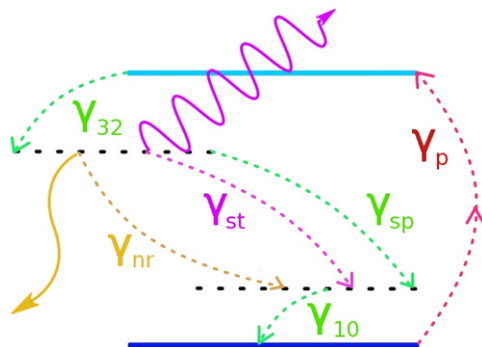
Figure 3. Schematic representation of the implemented 4-level laser rate equations. The electronic transitions (dashed lines) are due to 2-photon excitation γ_p, spontaneous decay γ_{sp}, non-radiative decay γ_{nr}, stimulated emission (pink line) γ_{st} and the transitions γ_{32} and γ_{10} which are necessary to derive a threshold behavior. The spontaneous emitted photon is not displayed here in the interest of clarity.

boundaries (see figure 2(c)). The full dissipative influence on coherent propagating photons and wave is found within the renormalized so -called mass term of the diffusion equation:

$$iD\xi^{-2} = -iD\chi_d^{-2} - c_1\left(\partial_Y^2 \Phi_{\epsilon\epsilon}(Q, \Omega)\right) + c_2 + iD\zeta^{-2}. \tag{5}$$

By solving the non-classical diffusion equation (5) the coefficients c_1 and c_2 are self-consistently derived, and we arrive the spatial distribution of energy density:

$$-\frac{\partial^2}{\partial Y^2}\Phi_{\epsilon\epsilon} = \frac{1}{D}\left[\frac{D}{-\chi_d^2} + \frac{D}{\zeta^2}\right]\Phi_{\epsilon\epsilon} + \text{ASE}. \tag{6}$$

The non-linear self-consistent microscopic random laser gain $\gamma_{21}n_2$ (see next section) incorporates the influences of both length scales χ_d and ζ,

$$\frac{D}{-\chi_d^2} + \frac{D}{\zeta^2} = \gamma_{21}n_2, \tag{7}$$

and therefore represents the physical properties of the random laser samples within the absorptive SI wafer. γ_{21} is the transition rate of stimulated emission and n_2 equals the self-consistent occupation of the upper laser level (see next section). The abbreviation ASE on the right of equation (6) represents all transport terms yielding amplified spontaneous emission.

4. Lasing and threshold behavior

Our diagrammatic transport approach as such is successful in explaining both strong and Anderson localization. We focus now on the implementation of a realistic semi-conductor ZnO which is able to perform a laser transition. In order to describe lasing action, the electronic dynamics have to be accounted for [24]. A popular way to do so is to consider an electronic system consisting of four energy levels and write down coupled equations for the occupation numbers of the individual energy levels (see figure 3). The resulting laser rate equations are given as
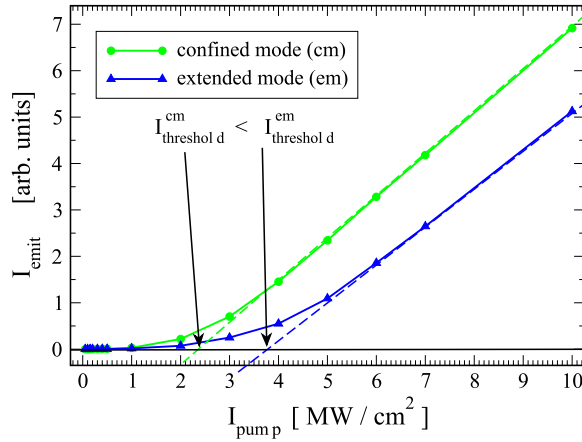
Figure 4. Laser dynamics and thresholds derived by the solution of the coupled system of mesoscopic transport and semiclassical time dependent laser rate equations taking into account energy conservation. Extended and confined modes (3.21 eV and 3.23 eV, see figure 2) are suffering different types of loss by means of transport and absorption, as well as spontaneous emission and nonradiative decay. The extended modes suffer in sum more, and therefore arrive at their laser thresholds for significantly higher pump intensities.

$$\frac{d}{dt}n_3(t) = \gamma_P - (1/\tau_{32})n_3$$

$$\frac{d}{dt}n_2(t) = (1/\tau_{32})n_3(t) - (1/\tau_{sp})n_2(t)$$

$$-(1/\tau_{21})[n_2(t) - n_1(t)]n_{Ph}(t) - (1/\tau_{nr})n_2(t)$$

$$\frac{d}{dt}n_1(t) = -(1/\tau_{10})n_1(t) + (1/\tau_{sp})n_2(t)$$

$$+ (1/\tau_{21})[n_2(t) - n_1(t)]n_{Ph}(t) + (1/\tau_{nr})n_2(t)$$

$$\frac{d}{dt}n_0(t) = (1/\tau_{10})n_1(t) - \gamma_p. \tag{8}$$

In the above equation (8), γ_P is the external pump rate, n_{0-3} are electronic populations of the levels respectively, τ_{ij} are the states' lifetimes $\frac{1}{\tau_{ij}} = \gamma_{ij}$, τ_{nr} is the non-radiative decay time, τ_{sp} represents the spontaneous decay time and τ_{21} is the time scale of the lasing transition. The term $[n_2(t) - n_1(t)]n_{Ph}(t)$ marks the inversion of the occupation numbers of level 1 and 2 proportional to the number of stimulated emitted photons n_{ph}. The spatial coordinates are suppressed in equation (8) for clarity of presentation.

The last and likeliest most crucial step is to couple the electron dynamics to the propagating photonic energy density. This is achieved by identifying the growth of the photonic energy density with a corresponding population inversion in the laser rate equation. The system is also solved dependent on time and the typical threshold behavior of the stimulated emitted photon number density is derived which matches the experiment for both lasing modes, confined as well as extended (see figure 4). Assuming 5.0 ns pulses the self-consistent laser threshold of the confined mode is derived to be ~2.4 $MW\ cm^{-2}$ while that of the extended mode is derived to be ~3.7 $MW\ cm^{-2}$.

5. Results and discussion

Numerical calculations of self-consistent photonic transport theory and random lasing lead to a variety of directly measurable quantities. Above all we mention that in disordered amplifying and constrained samples like the Si-confined ZnO powder here, the gain is clearly influenced by the boundary and consequently dependent on the position of measurement. This result leads to a locally changing refractive index which is an important point and has to be emphasized. It is a qualitative difference from previously existing self-consistent theories. The symmetry of mesoscopic transport is broken by the boundary condition, and the frequency dependent absorption in silicon leads to two qualitatively differing mode types. Strong confinement of a mode is in principle only possible when the symmetry in some dimension is unbroken.

A different situation leads inevitably to extended modes with diverse coherence properties. The computed correlation lengths ξ and intensity distributions of both types of modes can be found in figure 2. The correlation length is a measure for the mode size, which can be observed in the experiment.

In our calculations homogeneous dissipation for both mode types determined by the surface properties of the disordered sample is assumed to be less than 10% of the loss value through the same area of boundary. The boundaries are as such symmetric and determined by the underlying SI crystal substrate. The k-dependent absorption of SI can be found in [21]. The symmetric mode figure 2(b) suffers only homogeneous loss, is strongly confined due to self-consistent photon propagation throughout the system and obeys the dissipation induced length ζ. The stationary state diameter (derived at the decay of 1/e) in this case is $2.2 \times l_s$. Definitely fundamentally differently behaves the extended mode caused by spatial symmetry breaking (figure 2(c)), which consequently also results in a partial break of the time-reversal symmetry. The mode therefore obeys the dissipative length scale χ_d. Both lengths are deduced within equation 4. The denominator carries an inherent differential with respect to the limited dimension due to the broken symmetry through loss. With respect to the finite dimension, extended modes cover the whole extent of the sample. These modes are elliptically shaped, and the correlation length at the interface to the substrate is by far reduced when compared to the center.

A comparison of emitted intensity in spatial resolution figure 2(a) clearly shows that the extended laser mode obeys different laws than the confined mode does. The difference is obvious when comparing both profiles, the resticted y-dimension (blue dashed graph) and the wide x-dimension (solid lines). The aspect ratio is clearly of fundamental importance even though both directions are by far longer than the scattering mean -free path which is in both cases about $l_s = 500$ *nm* (for details see caption of figure 2). l_s is very short due to high self-consistent non-linearities. These non-linearities lead to a significantly different refractive index for pumped material compared to a result derived by CBS far below the threshold. The behavior can be explained in our model of coherent intensity propagation, which differs from the so-called quasi-mode model. In contrast to quasi-modes, which are deduced from a diagrammatic *single particle picture* of the electromagnetic wave, our results go much further. The correlation length ξ can be interpreted as a measure of the mode in the *correlated two particle picture*, i.e. the coherence of the wave and simultaneously the coherent transport of intensity. The interference contributions (Cooperons) suffer from dissipation, meaning the symmetry break in-plane especially reduces interference effects. Consequently the degree of coherence of transported intensity depicted in figure 2(b) is—apart from all spatial effects—below and at the

threshold much higher than in the situation of broken symmetry displayed in figure 2(c). This transport inherent coherence leads to a stronger accumulation of intensity but even more to higher non-linear gain. What this means is that the almost unlimited development of the Cooperon drives the system very fast to the lasing transition, which as such guarantees energy conservation in stationary state. In other words, Lethokovs bomb argument is avoided because the system prefers to lase.

In the case of extended modes, the situation changes. Cooperons are inhibited in their development due to the loss of the boundaries. Finally, it can be deduced that extended modes are preferentially built up by incoherent contributions and the accumulated intensity is locally renormalized by the loss through the boundary. In both cases Cooperon contributions remain the coherent stimulation process of emission. This positional distribution of the modes' coherent intensities are displayed in the color coding of figure 2(b) and (c). Corresponding laser thresholds to both mode types can be compared in figure 4. It can be clearly seen that the confined mode (green) reaches the threshold by far lower pumping intensity γ_p than the extended mode (blue) does. It is noted that this approach is in principle also usable to spatially overlapping as well as spectrally coupled laser switches [25] with an even more sophisticated mode coupling.

6. Conclusion

The solution of a complicated statistical behavior such as that of random lasing in granular disordered matter demonstrates the power of the Vollhardt–Wölfle transport theory of photons, which is coupled to laser rate equations self-consistently. The correlation length for the intensity at the laser transition derived by diagrammatic transport theory describes the modes' shapes and diameters and it includes the conditions of spatially uniform as well as time-reversal symmetry breaking losses. Engineering highly frequency -selective substrates is an efficient tuning mechanism for spectrally very close modes which arise at different thresholds and arrive at completely different shapes and diameters due to the breaking of the spatial symmetry. Confined modes exist due to unbroken spatial symmetry, while extended modes arise due to spatially non-uniform position-dependent losses and non-linearities. The conception of the mode we derive in this work is fundamentally different from the quasi-mode picture, which is a single-particle picture result. Our theory defines the lasing modes as correlations between scattered photons. The results presented here for lasing mode diameters are inseparable from the two-particle picture and they are a measure of coherent transported intensity in granular amplifying media at the laser threshold. A breaking of positional symmetry leads both to the formation of extended modes and also to their pinning. It has to be pointed out that the aspect ratio of the sample is relevant for the modes' shapes, even though the samples are by far larger in every extent than the scattering mean -free path. Additionally a symmetry break due to loss leads to significantly differing lasing threshold behavior, varying gain and gain-saturation dynamics. We hope that these results stimulate further research, theoretically and experimentally, on the modal behavior of random lasers.

Acknowledgements

References

[1] Cao H, Xu J Y, Zhang D Z, Chang S H, Ho S T, Seelig E W, Liu X and Chang R P H 2000 Spatial confinement of laser light in active random media *Phys. Rev. Lett.* **84** 5584

[2] Vanneste C and Sebbah P 2001 Selective excitation of localized modes in active random media *Phys. Rev. Lett.* **87** 183903

[3] Mujumdar S, Ricci M, Torre R and Wiersma D S 2004 Amplified extended modes in random lasers *Phys. Rev. Lett.* **93** 053903

[4] Vanneste C, Sebbah P and Cao H 2007 Lasing with resonant feedback in weakly scattering random systems *Phys. Rev. Lett.* **98** 143902

[5] El-Dardiry R G S, Mosk A P, Muskens O and Lagendijk A 2010 Experimental studies on the mode structure of random lasers *Phys. Rev.* A **81** 043830

[6] Stano P and Jacquod P 2013 Overlapping lasing modes in the Anderson localized regime *Nat. Photon.* **7** 66–71

[7] Türeci H E, Ge L, Rotter S and Stone A D 2008 Strong interactions in multimode random lasers *Science* **320** 643

[8] Leonetti M, Conti C and Lopez C 2011 The mode-locking transition of random lasers *Nat. Photon.* **5** 615

[9] van der Molen K L, Tjerkstra R W, Mosk A P and Lagendijk A 2007 Spatial extent of random laser modes *Phys. Rev. Lett.* **98** 14901

[10] Polson R C and Vardeny Z V 2010 Spatially mapping random lasing cavities *Opt. Lett.* **35** 2801

[11] Fallert J, Dietz R J B, Sartor J, Schneider D, Klingshirn C and Kalt H 2009 Co-existence of strongly and weakly localized random laser modes *Nat. Photon.* **3** 279

[12] Kalt H, Fallert J, Dietz R J B, Sartor J, Schneider D and Klingshirn C 2010 Random lasing in nanocrystalline ZnO powders *Phys. Stat. Sol.* b **247** 1448

[13] Vollhardt D and Wölfle P 1980 Diagrammatic, self-consistent treatment of the Anderson localization problem in $d < = 2$ dimensions *Phys. Rev.* B **22** 4666

[14] Akkermans E and Maynard R 1985 Weak localization of waves *J. Phys. Lett.* **46** 1045

[15] Yamilov A G, Sarma R, Redding B, Payne B, Noh H and Cao H 2014 Position-dependent diffusion of light in disordered waveguides *Phys. Rev. Lett.* **112** 023904

[16] Apalkov V M, Raikh M E and Shapiro B 2002 Random resonators and prelocalized modes in disordered dielectric films *Phys. Rev. Lett.* **89** 016802

[17] Andreasen J and Cao H 2010 Numerical study of amplified spontaneous emission and lasing in random media *Phys. Rev.* A **82** 063835

[18] Frank R and Lubatsch A 2011 Scalar wave propagation in random amplifying media: influence of localization effects on length and time scales and threshold behavior *Phys. Rev.* A **84** 013814

[19] Lubatsch A, Kroha J and Busch K 2005 Theory of light diffusion in disordered media with linear absorption or gain *Phys. Rev.* B **71** 184201

[20] Maret G, Sperling T, Buehrer W, Lubatsch A, Frank R and Aegerter C M 2013 Reply to comment by F Scheffold and D Wiersma: inelastic scattering puts in question recent claims of Anderson localization of light *Nat. Photon.* **7** 934–5

[21] Palik E D 1997 *Handbook of Optical Constants* (Amsterdam: Elsevier)

[22] Mie G 1908 Beiträge zur Optik trüber Medien, speziell kolloidaler Metallösungen *Ann. Phys.* **4** 377–445

[23] van der Molen K L, Zijlstra P, Lagendijk A and Mosk A P 2006 Laser threshold of Mie resonances *Opt. Lett.* **31** 1432

[24] Florescu L and John S 2004 Lasing in a random amplifying medium: spatiotemporal characteristics and nonadiabatic atomic dynamics *Phys. Rev.* E **70** 036607

[25] Leonetti M, Conti C and Lopez C 2012 Tunable degree of localization in random lasers with controlled interaction *Appl. Phys. Lett.* **101** 051104